EFFECT OF HEAT TREATMENT ON THERMAL CONDUCTIVITY OF ADDITIVELY MANUFACTURED AISI H13 TOOL STEEL

[1]Samo TOME, [2]Blaž KARPE, [1]Irena PAULIN, [1]Matjaž GODEC

[1]Institute of Metals and Technology, Ljubljana, Slovenia, EU,
samo.tome@imt.si
[2]University of Ljubljana, Faculty of Natural Sciences and Engineering, Ljubljana, Slovenia, EU

https://doi.org/10.37904/metal.2023.4677

Abstract

AISI H13 is commonly used for tooling, where higher wear resistance, thermal fatigue resistance, or hot toughness is required. Such examples include forging dies, plastic molds, hot shear blades, high-pressure die casting, and extrusion dies. Thus, thermal conductivity is one of the most important factors for hot work tools. Typically, the work cycle of a hot work tool designed for forging consists of four main phases: the forging stroke, with which the die imparts its shape onto the part, a brief pause while the die is reset to its original position, a lubrication phase, and a post lubrication dwell phase. During the forging phase, a significant amount of heat is transferred to the die while it is in contact with the part. This heat must then be dispelled for the part to return to a working temperature. While somewhat different, other hot work processes mentioned above are similar in that the hot work tool gets heated to a high temperature due to the contact with the object of deformation. The process of additive manufacturing (AM) promises better, more efficient tool production with features like conforming cooling channels, which would reduce the thermal fatigue of tools, prolonging tool life. However, the powder bed fusion (PBF) method creates a columnar microstructure, which has a detrimental effect on the thermal conductivity of H13 tool steel. Our investigation focused on the beneficial effect of heat treatment, specifically annealing at different temperatures, on the thermal conductivity of AM-produced H13 parts.

Keywords: SLM, Thermal Conductivity, Tool Steel, Heat Treatment

1. INTRODUCTION

Additive manufacturing (AM) is a new chapter of metallurgy. It can offer efficiently produced parts with relative precision in the right application. Due to these factors, AM is fast becoming a staple manufacturing process in aeronautics and medicine, however, its potential in die-making should not be overlooked. A big selling point of AM is the ability to manufacture complex geometries, which would not be possible with conventional means. Of the various AM methods, Laser Powder Bed Fusion (LPBF) is one of the most promising.

The LPBF process is a layer-by-layer printing process, with 3 main steps: First, an applicator, such as a brush, applies a thin layer (typically 20 - 60 μm thick) of metal powder onto the base plate. A laser beam then melts the freshly applied layer of powder in the shape of the part, and the base plate is lowered, so a new layer of powder can be applied. This process is repeated until a full part is formed. While other methods like direct energy deposit (DED) struggle with sharp corners and thin wall sections, LPBF offers excellent spatial resolution, with low material waste [1,2].

Thermal conductivity plays a large part in the applicability of tool steel as dies for various hot work processes. Depending on the use, hot work steel dies can be exposed to a wide range of temperatures. On the lower end is plastic injection molding, where the die temperature rarely exceeds 100 °C [3-5]. On the high end is hot forging, where during the dwell time, when the tool is in contact with the heated material, the tool can reach a peak temperature of around 700 °C. It is then followed, by rapid cooling, due to the application of lubricant, cooling it down to about 200 - 350 °C [6-8]. The large amplitude of such heating and cooling cycles causes thermal fatigue, which shortens the lifespan of tools. With higher thermal conductivity, the amplitude is smaller, thus ensuring longer tool life. This is why it's imperative for AM-manufactured tools to maintain the same level of thermal conductivity as conventionally produced tools.

2. MATERIALS AND METHODS

The powder used to make the samples was a gas-atomized H13 powder with its chemical composition given in **Table 1**. An Aconity 3D MINI (Aconity Gmbh, Herzogenrath, Germany) LPBF machine was used to produce two cylinders of 40 mm diameter with 15 mm height as seen in **Figure 1**, along with a smaller 15 mm diameter with 10 mm height sample to determine the microstructure of the as-built samples. The samples were manufactured with a power of 250 W, scanning speed of 347 mm/s, layer thickness of 30 µm, hatch spacing of 60 µm, laser beam diameter of 60 µm and 200 °C of base plate preheating. Reference samples were produced from a steel bar, manufactured via classical means (cast, forged, and soft annealed). The flat surface of all the samples was ground, to ensure that there were no air pockets on the interface between the samples. Thermal conductivity was measured with a Hot disk TPS 2200 (Hot Disk AB, Gothenburg, Sweden). A Kapton-insulated sensor was placed between the base of both samples, then the samples were left to acclimate to 23 °C to ensure an accurate measurement. The power for the test was set at 0.75, 1, and 1.25 W, and the measuring time was 5s. From the measurements, average thermal conductivity was calculated. The AM samples were then tempered, and the measurements were performed again. In all, 8 sets of measurements were performed, for the different states of the steel:

- Reference sample (soft annealed, conventionally produced H13).
- AM sample (as-built state).
- AM annealed at 450 °C for 1h.
- AM annealed at 500 °C for 1h.
- AM annealed at 550 °C for 1h.
- AM annealed at 600 °C for 1h.
- AM annealed at 650 °C for 1h.
- AM soft annealed at 800 °C for 1h.

Table 1 Chemical composition of the H13 powder

Elements (wt%)	C	Si	Mn	S	Cr	Ni	Cu	Mo	V	Fe
	0.42	0.94	0.42	0.007	5.10	0.055	0.011	1.60	1.11	Bal.

The samples for microstructural investigation were cut along the build direction, mounted in Bakelite resin then ground, polished, and etched using Villela's reagent (1 gram of picric acid and 5 ml hydrochloric acid

to 100 ml of ethanol) to reveal the microstructure. The samples were observed under a light microscope (Nikon Microphot-FXA, Nikon, Tokyo, Japan) equipped with an Olympus DP73 digital camera (Olympus, Tokyo, Japan) and a ZEISS CrossBeam 550 FIBSEM (ZEISS, Oberkochen, Germany) scanning electron microscope to determine the porosity and microstructure of the samples. AM sample density was measured using the Archimedes method, with all the samples having a higher density than 99 %.

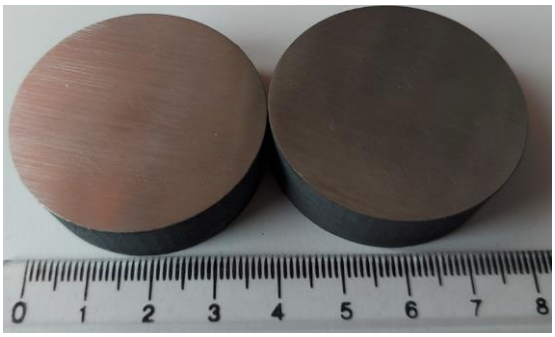

Figure 1 Additively manufactured samples

3. RESULTS AND DISCUSSION

The microstructure of the as-built samples consists mainly of martensite, with practically no visible carbides. The stand-out feature is the scan tracs left behind by the laser (**Figure 2**). Sometimes referred to as melt pools, these alternating bands are tempered, and untampered martensite, formed by the remelting of higher-up layers during printing [9,10]. **Figures 3a) and b)** show secondary electron images of the as-built as well as the soft annealed states. The melt pools and the columnar grain structure are typical for AM parts and are still clearly visible. There is also a distinct lack of carbides in **Figure 3c)** as opposed to the soft annealed sample (**Figure 3d)**), due to all the carbide-forming elements being dissolved in the steel matrix.

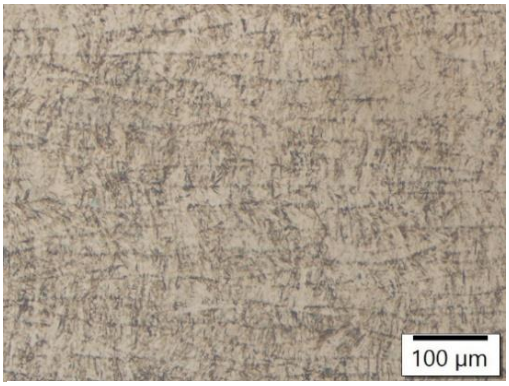

Figure 2 Melt pools formed by the LPBF process

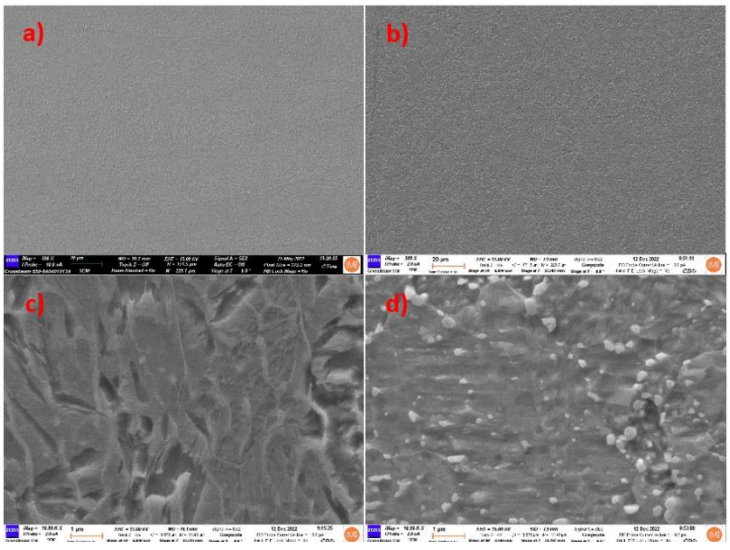

Figure 3 SEM images showing the a) melt pools and columnar grain structure in the AM sample, b) the microstructure of conventionally produced AISI H13 in the soft annealed state, c) the martensitic microstructure of the AM sample, with few to no carbides, d) the soft annealed microstructure of the conventionally produced AISI H13, which has many carbides.

Our baseline for thermal conductivity was conventionally produced AISI H13 in the soft annealed state. It had a thermal conductivity of 25.61 W/mK. The as-built samples had the lowest thermal conductivity, with a value of 17.57 W/mK. Annealing the samples at 450 °C improved their thermal conductivity to a value of 18.16 W/mK. Annealing at higher temperatures (500 °C, 550 °C, 600 °C, 650 °C and 800 °C) further improved the thermal conductivity to 18.60 W/mK, 19.86 W/mK, 21.05 W/mK, 23.18 W/mK and 24.41 W/mK respectively. These values are shown in **Figure 4**. The main factor in the change of thermal conductivity is the precipitation of carbides. Due to the rapid cooling and solidification associated with the LPBF process, most of the carbide-forming elements (Cr, V, Mo) remain dissolved in the matrix. This distorts the matrix, making it more difficult for heat to travel through the material. When the solid solution is annealed, the solute elements begin to defuse and precipitate in the form of carbides. As a result, the matrix strain is relaxed, and thermal conductivity increases. [11-13] However, there is still a notable difference in the thermal conductivity of soft annealed samples produced by different methods. This is due to the porosity of the AM samples (**Figure 5**). While a high density of greater than 99% was achieved with these samples, some porosity remains, causing the loss in thermal conductivity.

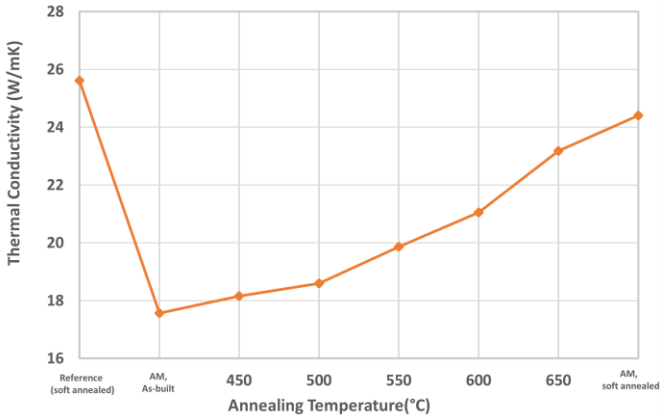

Figure 4 Thermal conductivity of AISI H13 depending on the heat treatment

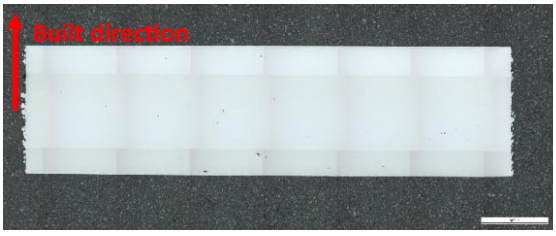

Figure 5 cross-section of the AM-produced sample

4. CONCLUSION

Thermal conductivity was measured for LPBF-manufactured samples in as-built, tampered, and soft annealed states, along with a reference sample produced by conventional means. The as-built sample has significantly lower thermal conductivity than the reference material. With rising annealing temperatures, thermal conductivity recovers, however, it never achieves the same value as the conventionally produced material. The difference is mainly attributed to porosity, as the microstructure after soft annealing is simmilar that of conventionally produced H13.

ACKNOWLEDGEMENTS

This work was carried out within the framework of the Slovene program P2-0132 and project L2-2613 of the Slovenian Research Agency (ARIS).

REFERENCES

[1] LALEGANI DEZAKI, M.; SERJOUEI, A.; ZOLFAGHARIAN, A.; FOTOUHI, M.; MORADI, M.; ARIFFIN, M.K.A.; BODAGHI, M. A review on additive/subtractive hybrid manufacturing of directed energy deposition (DED) process. *Adv. Powder Mater.* 2022, vol. 1, 100054. Available from: https://doi.org/10.1016/j.apmate.2022.100054.

[2] NARVAN, M.; AL-RUBAIE, K.S.; ELBESTAWI, M. Process-structure-property relationships of AISI H13 tool steel processed with selective laser melting. *Materials (Basel).* 2019, vol. 12, 2284. Available from: https://doi.org/10.3390/ma12142284.

[3] OZCELIK, B.; ERZURUMLU, T. Comparison of the warpage optimization in the plastic injection molding using ANOVA, neural network model, and genetic algorithm. *J. Mater. Process. Technol.* 2006, vol. 171, pp. 437-445. Available from: https://doi.org/10.1016/J.JMATPROTEC.2005.04.120.

[4] NIAN, S.C.; WU, C.Y.; HUANG, M.S. Warpage control of thin-walled injection molding using local mold temperatures. *Int. Commun. Heat Mass Transf.* 2015, vol. 61, pp. 102-110. Available from: https://doi.org/10.1016/J.ICHEATMASSTRANSFER.2014.12.008.

[5] SHEN, C.; WANG, L.; LI, Q. Optimization of injection molding process parameters using combination of artificial neural network and genetic algorithm method. *J. Mater. Process. Technol.* 2007, vol. 183, pp. 412-418. Available from: https://doi.org/10.1016/J.JMATPROTEC.2006.10.036.

[6] BEHRENS, B.A.; BOUGUECHA, A.; LÜKEN, I.; MIELKE, J.; BISTRON, M. Tribology in Hot Forging. *Compr. Mater. Process.* 2014, vol. 5, pp. 211-234. Available from: https://doi.org/10.1016/B978-0-08-096532-1.00538-0.

[7] HAWRYLUK, M.; ZIEMBA, J. Possibilities of application measurement techniques in hot die forging processes. *Measurement.* 2017, vol. 110, pp. 284-295. Available from: https://doi.org/10.1016/J.MEASUREMENT.2017.07.003.

[8] BARRAU, O.; BOHER, C.; GRAS, R.; REZAI-ARIA, F. Analysis of the friction and wear behaviour of hot work tool steel for forging. *Wear.* 2003, vol. 255, pp. 1444-1454. Available from: https://doi.org/10.1016/S0043-1648(03)00280-1.

[9] WANG, M.; LI, W.; WU, Y.; LI, S.; CAI, C.; WEN, S.; WEI, Q.; SHI, Y.; YE, F.; CHEN, Z. High-Temperature Properties and Microstructural Stability of the AISI H13 Hot-Work Tool Steel Processed by Selective Laser Melting. *Metall. Mater. Trans. B Process Metall. Mater. Process. Sci.* 2019, vol. 50, pp. 531-542.

[10] SUN, Y.; WANG, J.; LI, M.; WANG, Y.; LI, C.; DAI, T.; HAO, M.; DING, H. Thermal and mechanical properties of selective laser melted and heat treated H13 hot work tool steel. *Mater. Des.* 2022, vol. 224, 111295. Available from: https://doi.org/10.1016/J.MATDES.2022.111295.

[11] SIMMONS, J.C.; CHEN, X.; AZIZI, A.; DAEUMER, M.A.; ZAVALIJ, P.Y.; ZHOU, G.; SCHIFFRES, S.N. Influence of processing and microstructure on the local and bulk thermal conductivity of selective laser melted 316L stainless steel. *Addit. Manuf.* 2020, vol. 32, 100996. Available from: https://doi.org/10.1016/J.ADDMA.2019.100996.

[12] PEET, M.J.; HASAN, H.S.; BHADESHIA, H.K.D.H. Prediction of thermal conductivity of steel. *Int. J. Heat Mass Transf.* 2011, vol. 54, pp. 2602-2608, Available from: https://doi.org/10.1016/J.IJHEATMASSTRANSFER.2011.01.025.

[13] KLEIN, S.; MUJICA RONCERY, L.; WALTER, M.; WEBER, S.; THEISEN, W. Diffusion processes during cementite precipitation and their impact on electrical and thermal conductivity of a heat-treatable steel. *J. Mater. Sci.* 2016, vol. 52, pp. 375-390. Available from: https://doi.org/10.1007/S10853-016-0338-1.